CAPACITY OF MULTI-ANTENNA ARRAY SYSTEMS IN INDOOR WIRELESS ENVIRONMENT

Chen-Nee Chuah, Joseph M. Kahn and David Tse
211-27 Cory Hall, University of California Berkeley, CA 94720
e-mail: {chuah, jmk, dtse}@eecs.berkeley.edu

Abstract

Studies show that multiple-element antenna arrays (MEA) with n transmitters and n receivers can achieve n more bits/Hz than single-antenna systems in an independent Rayleigh fading environment. In this paper, we explore the behavior of MEA capacities in a more realistic propagation environment simulated via the WiSE ray tracing tool. We impose an average power constraint and collect statistics of the capacity, C_{wf} and mutual information I_{eq}. In addition, we derive mathematically the asymptotic growth rates C_{wf}/n and I_{eq}/n as $n \to \infty$ for two cases: (a) independent fadings and (b) spatially correlated fadings between antennas. C_{wf}/n and I_{eq}/n converge to constants C_{wf}* and I_{eq}*, respectively in case (a), and to C_{wf}^{o} and I_{eq}^{o} in case (b). C_{wf}^{o} and I_{eq}^{o} predict very closely the slope observed in simulations, even at moderate n = 16.

I. Introduction

The signals propagating through the wireless channel experience path loss and distortion due to multipath fading and additive noise. These impairments, along with the constraints of power and bandwidth, limit the system capacity. In the past, multiple antennas are used at the receiver to combat multipath fading of the desired signal, e.g. maximal ratio combining mentioned in [1], or to suppress interfering signals, e.g. optimal combining in [2]. Recent studies report that using MEAs at both ends delivers significantly higher bit-rates than single-antenna systems ([3], [4]). In [4], Foschini and Gans consider n transmitting and n receiving antennas, with i. i. d. narrowband Rayleigh fading between antenna pairs. Assume that power is allocated equally over all transmitters, the MEA mutual information (I_{eq}) is reported to grow linearly with n for a given fixed average transmitter power. An MEA system achieves almost n more bits/Hz for every 3 dB increase in signal-to-noise ratio (SNR), compared to the single antenna case, which only achieves one additional bit/Hz.

In practice, correlation exists between the signals transmitted by or received at different antennas. Correlation may arise if the antenna elements are not spaced far apart enough, e.g., Lee pointed out in [5] that the required antenna spacing to obtain correlation coefficient between signals to be less than 0.7 is approximately 70 wavelengths for broadside case and 15-20 wavelengths for inline case. The presence of a dominant line-of-sight component can also affect the MEA capacities.

The first goal of this paper is to explore the MEA capacities in a more realistic propagation environments where the fadings are not necessarily Rayleigh nor independent. Our work seeks to determine the capacity C_{wf} when *the transmitter knows the channel* and *optimum power allocation* (*water-filling*) is used. Secondly, we compute the mutual information I_{eq} with *equal power allocation* of the MEA system and investigate the performance degradation when compared to C_{wf}.

We study the behavior of MEA capacities through simulation and analysis. For simulation, we use the WiSE (Wireless System Engineering)[1] [6] software tool to model explicitly the channel response between a transmitter and a receiver placed inside an office building. For analysis, we model the multiple-input-multiple-output (MIMO) Rayleigh-fading channel as a matrix H. We study how C_{wf} and I_{eq} behave as n grows large. We show almost sure convergence of the asymptotic growth rate C_{wf}/n and I_{eq}/n considering two cases: (a) when fadings between different antenna pairs are independent and (b) when these fadings are correlated.

The remainder of this paper is organized as follows. In Section II, we model the channel as a MIMO system with flat frequency response. Using this mathematical model in Section III, we present information-theoretic results for the capacity of MEA systems and analyze its asymptotic growth rate as n grows large. In Section IV, we present capacity estimates for the simulated channels and discuss the discrepancies between these results and the asymptotic capacities predicted by theory. We briefly describe how WiSE is used to represent the indoor propagation environment that our study is based on. Conclusions are presented in Section V.

II. Channel Model

The following notation will be used throughout the paper: $'$ for vector transpose, † for transpose conjugate, I_n for the $n \times n$ identity matrix, $E[\cdot]$ for expectation, and underline for vectors.

A. Basic Channel Model

We consider a single-user, point-to-point communication channel with n transmitting and n receiving antennas, with no co-channel interference. We assume that the channel response is flat over frequency. This approximation is reasonable if the communication band-

[1] WiSE is a ray tracing tool that predicts RF propagation in a specific building, based on off-line experimental measurements.

width, W, is much less than the coherent bandwidth. In our simulated channels, the maximum delay spread[1] is 24 ns. The coherence bandwidth is approximately the reciprocal of the delay spread, which is 42 MHz. Therefore the frequency response can be considered flat as long as W is much less than 40 MHz.

We assume that the channel is linear time-invariant and use the following discrete-time equivalent model:

$$\underline{Y} = H\underline{X} + \underline{Z} \quad (1)$$

$\underline{X} = [x_1, x_2, \ldots, x_T]'$ is an $n \times 1$ vector whose jth component represents the signal transmitted by the jth antenna. Similarly, the received signal and received noise are represented by $n \times 1$ vectors, $\underline{Y}$ and $\underline{Z}$, respectively, where y_i and z_i represent the signal and noise received at the ith antenna. The complex path gain between transmitter j and receiver i is represented by H_{ij}, for i = 1, 2, ..., n and j = 1, 2, ..., n. We further assume that:

- The total radiated power is P_{tot}, regardless of n.
- The noise $\underline{Z}$, is an additive white complex Gaussian random vector. Its components, Z_i, i = 1, 2, ..., n, are i. i. d. circularly symmetric complex Gaussian random variables with variance $E[|Z_i|^2] = N_0W$.

We consider the following two cases:

1. H is known only to the receiver but not the transmitter. Power is distributed equally over all transmitting antennas in this case.
2. H is known at the transmitter and receiver. Therefore, power allocation can be optimized to maximize the achievable rate over the channel.

In this work, we treat H as quasi-static. H is considered fixed for the whole duration of communication, thus capacity is computed for each realization of H without time averaging. On the other hand, H changes if the receiver is moved from one place to the other, which happens over a much larger time scale. The capacity C_{wf} and mutual information I_{eq} associated with H can be viewed as random variables.

III. Analysis of MEA Capacities

Channel capacity is defined as the highest rate at which information can be sent with arbitrarily low probability of error [8]. Since H is quasi-static, it is reasonable to associate C_{wf} to a specific realization of H, for a fixed P_{tot} and N_0W. Throughout our analysis, we assume H_{ij} for i, j = 1, 2,..., n, are identically distributed with the same variance $\upsilon^2 = E[|H_{ij} - E[H_{ij}]|^2]$. We assume that υ^2 is the same for all fading gain H_{ij} for all positions of the transmitting and receiving MEAs within their respective work spaces.

[1] Delay spread here refers to the difference between the arrival time of the earliest strong ray and the last strong ray that arrive at the receiver.

When n antennas are used, we denote the MEA capacity and mutual information as $C_{\text{wf}}(n)$ and $I_{\text{eq}}(n)$, respectively. For the case with n = 1, the capacity is:

$$C_{\text{wf}}(1) = I_{\text{eq}}(1) = \log_2\left(1 + \frac{P_{\text{tot}}}{N_0W}|H|^2\right) \text{ bps/Hz.} \quad (2)$$

In the high-SNR regime, each 3-dB increase of P_{tot}/N_0W yields a capacity increase of 1 bps/Hz.

A. Capacity With Water-filling Power Allocation

In this section, we assume the transmitter has perfect knowledge about the channel. Thus, P_{tot} can be allocated most efficiently over the different transmitters to achieve the highest possible bit rate, which is given by:

$$C_{\text{wf}}(n) = \max_{Q} \log_2 \det\left[I_n + \frac{HQH^\dagger}{N_0W}\right] \text{ bps/Hz,} \quad (3)$$

where Q is the $n \times n$ covariance matrix of $\underline{X}$ ($Q = E[\underline{X}\underline{X}^\dagger]$), and must satisfy the average power constraint:

$$\text{tr}(Q) = \sum_{i=1}^{n} E[\underline{X}_i^2] \le P_{\text{tot}}. \quad (4)$$

The achievable capacity ([9]) is:

$$C_{\text{wf}}(n) = \sum_{i=1}^{n} \log_2(\Lambda_i\mu)^+ , \quad (5)$$

where μ satisfies $\sum_i \left(\mu - \frac{1}{\Lambda_i}\right)^+ = P_{\text{tot}}$,

and Λ_i's are the eigenvalues of $HH^\dagger$.

The optimal solution that gives the capacity in (5) is analogous to the water-filling solutions for parallel Gaussian channels [8].

B. Mutual Information With Equal Power Allocation

Here, we assume that equal power is radiated from each transmitting antenna, which is a natural thing to do when the transmitter does not know the channel. The MEA mutual information is:

$$I_{\text{eq}}(n) = \log_2 \det\left[I_n + \left(\frac{P_{\text{tot}}}{nN_0W}\right) \cdot HH^\dagger\right] \text{ bps/Hz.} \quad (6)$$

C. Asymptotic Behavior of Capacity

We investigate the growth of I_{eq} and C_{wf} as n grows large for two cases: (a) when path gains, H_{ij}, are independent, and (b) when H_{ij}'s are correlated. In both cases, we assume that H_{ij}'s are identically distributed complex Gaussian with variance υ^2. We define the average received SNR as $\rho = \upsilon^2 P_{\text{tot}}/N_0W$.

1. Assuming Independence of Path Gains

For a given H, the capacity of n-antenna MEA is given by (5). The Λ_i's are random variables that depend on H. For each n, let F_n be the fraction of Λ_i less than or equal to Λ with n antennas:

$$F_n(\Lambda) = \frac{1}{n}\left|\{i:(\Lambda_i \le \Lambda)\}\right|. \quad (7)$$

Note that I_{eq} and C_{wf} depend on H only through the empirical distribution of Λ_i, $F_n(\Lambda)$. The asymptotic properties of $C_{wf}(n)$ depends on how the distribution F_n behaves as n approaches infinity. Khorunzhy et al, and Yin studied convergence of F_n in [10]-[11]. The following almost sure convergence theorem is due to the work by Silverstein et al in [12].

Theorem 1. Define $G_n(\Lambda) := F_n(n\Lambda)$. Then, almost surely, G_n converges to a nonrandom distribution G*, which has a density given by:

$$g^*(\Lambda) = \begin{cases} \frac{1}{\pi}\sqrt{\frac{1}{\Lambda} - \frac{1}{4}} & 0 \le \Lambda \le 4 \\ 0 & \text{otherwise.} \end{cases} \quad (8)$$

The scaling by n in the definition of F_n means that the Λ_i are growing as order n. After rescaling, the distribution converges to a deterministic limiting distribution, i.e. for large n, $F_n(n\Lambda)$ looks similar for almost all realization of H. Using this theorem, we derive the asymptotic growth rate of $C_{wf}(n)$ as $n \to \infty$ while keeping the average received SNR ρ constant.

Proposition 1. With almost sure convergence,

$$\frac{C_{wf}(n)}{n} \to C_{wf}^*(\rho), \text{ where}$$

$$C_{wf}^*(\rho) = \int_0^4 (\log_2(\mu\Lambda))^+ \cdot g^*(\Lambda)\, d\Lambda \quad (9)$$

and μ satisfies $\int_0^4 \left(\mu - \frac{1}{\Lambda}\right)^+ \cdot g^*(\Lambda)\, d\Lambda = \rho$.

If we assume the transmitter always allocates an equal power P_{tot}/n to each transmitting antenna, the mutual information is given by (6). Using Theorem 1, we can prove the following proposition.

Proposition 2. With almost sure convergence,

$$\frac{I_{eq}(n)}{n} \to I_{eq}^*(\rho), \text{ where}$$

$$I_{eq}^*(\rho) = \int_0^4 (\log_2(1 + \alpha\Lambda))^+ \cdot g^*(\Lambda)\, d\Lambda. \quad (10)$$

With the above two propositions, we find that $C_{wf}(n)$ and $I_{eq}(n)$ scale like nC_{wf}^* and nI_{eq}^*, respectively. Using L'Hopital's rule, it can be shown that at low SNR,

$$\lim_{\rho \to 0} \frac{C_{wf}^*}{I_{eq}^*} = 4,$$

while at high SNR, $\lim_{\rho \to \infty} C_{wf}^* - I_{eq}^* = 0$.

2. Considering Correlation between Path Gains

Let Ψ^T be an $n \times n$ matrix whose entry Ψ^T_{jk} is the correlation coefficient between signals transmitted by jth antenna and kth antenna,

$$\Psi^T_{jk} = E[H_{pj}H_{pk}^*] / \sqrt{E[|H_{pj}|^2]E[|H_{pk}|^2]}. \quad (11)$$

In our model, we assume that Ψ^T_{jk} does not depend on the index of the receiving antenna, i.e. p can be arbitrary as long as $p \in \{1, 2, \ldots, n\}$. Similarly, let Ψ^R be an $n \times n$ matrix whose entry Ψ^R_{pq} is the correlation between signals at receiver p and receiver q,

$$\Psi^R_{pq} = E[H_{pj}H_{qj}^*] / \sqrt{E[|H_{pj}|^2]E[|H_{qj}|^2]}, \quad (12)$$

and it is also assumed to be independent of the index of the transmitting antenna, j.

To simplify our analysis, we assume that correlation for H_{ij}'s when both transmitting and receiving antennas are different is the product of the two one-dimensional correlation function mentioned above:

$$E[H_{pj}H_{qk}^*] / \sqrt{E[|H_{pj}|^2]E[|H_{qk}|^2]} = \Psi^R_{pq} \cdot \Psi^T_{jk}. \quad (13)$$

We verify the validity of this assumption through WiSE simulation. We estimate correlation of H_{ij}'s empirically from 1000 realizations of H for $n = 2$. Comparing the product of Ψ^T_{12} and Ψ^R_{12} with the actual estimate of $E[H_{11}H_{22}^*]$, close agreement is found consistently between the two over the range of d that we consider.

The asymptotic results in previous section can be extended to the case when the H_{ij}'s are correlated, under certain assumptions on the covariance matrices Ψ^R and Ψ^T. In particular, we assume that the empirical distributions of the eigenvalues of Ψ^R and Ψ^T converge to some limiting distributions F_R and F_T, respectively. This will be true if:

- the correlation between the fading at two antennas depends only on the relative and not absolute positions of the antennas; and
- the antennas are arranged on a regular lattice, such as in square grids or linear arrays, and as we scale up the number of antennas, the relative positions of adjacent antennas are fixed.

Under the above conditions, it can be shown that almost surely, as $n \to \infty$,

$$\frac{C_{wf}(n)}{n} \to C_{wf}^o(F_R, F_T, \rho) \quad (14a)$$

$$\text{and } \frac{I_{eq}(n)}{n} \to I_{eq}^o(F_R, F_T, \rho), \quad (14b)$$

where C_{wf}^o and I_{eq}^o are constants that depend only on the SNR and the limiting eigenvalues distributions of Ψ^R and Ψ^T. While these limits can be computed for arbitrary SNR [13], we shall focus here only on the case when the SNR is high. In this regime, particular simple expres-

sions can be obtained. It can be shown that at high SNR,

$$C_{wf}^{o}(F_R, F_T, \rho) \approx I_{eq}^{o}(F_R, F_T, \rho) \quad (15)$$
$$\approx \log_2\rho + \int_0^1 \log_2\eta^R(x)dx$$
$$+ \int_0^1 \log_2 F_T^{-1}(x)dx$$

where for each x, $\eta^R(x)$ is the unique solution to:

$$\int_0^1 \frac{F_R^{-1}(y)}{\eta^R(x) + xF_R^{-1}(y)}dy = 1. \quad (16)$$

The approximation in (15) is in the sense that the difference goes to zero as $\rho \to \infty$. It is shown in [13] that

$$\int_0^1 \log_2\eta^R(x)dx \le -1, \quad (17)$$

with equality if and only if fadings are independent at the receiver. Hence this term quantifies the capacity penalty due to correlation at the receiver. It can also be shown that

$$\int_0^1 \log_2 F_T^{-1}(x)dx \le 0, \quad (18)$$

with equality if and only if fadings are independent at the transmitter. This term thus quantifies the capacity penalty due to correlation at the transmitter.

IV. Ray-Tracing Channel Simulation

A. WiSE System Model

We use the experimentally based WiSE ray tracing simulator [6] to generate the channel matrix H for the indoor wireless environment of a two-floor office building in New Jersey (see Fig. 1). We place the transmitting MEA on the first floor ceiling near the middle of the office building throughout our study. Receiving MEAs are placed with random rotations at 1000 randomly chosen positions in Room A, which is at intermediate distance from the transmitter. We consider a carrier frequency of 5.2 GHz (wavelength, λ = 0.58 cm). The MEAs consist of multiple omnidirectional antennas, arranged either in square grids or linear arrays within horizontal planes. The separation between antenna elements d is the same for both the transmitting and receiving MEAs.

Since H varies for different receiver locations, we estimate the channel variance υ^2, by averaging over 1000 realizations of H, and over all possible antenna pairs, j to i. We assume that the average received SNR ρ, as defined in Section III-C, should be high enough for low-error-rate communication. If SNR is too low, we need long codes to provide enough redundancy to combat the noise so that we can recover the desired signal with low error probability at the receiver. The practical constraints on A/D converters that are available with current technology limit the maximum SNR that can be exploited effectively. Thus, we consider SNRs in the 18-22 dB range. For all our simulations, we assume W to be 10 MHz, and N_0 to be -170 dBm/Hz[1], giving a total noise variance N_0W of -100.8 dBm. The capacity and mutual information, $C_{wf}(n)$ and $I_{eq}(n)$, are computed for different n.

B. Simulation Results and Discussion

1. Capacity and Mutual Information of MEAs

In this section, we consider square arrays for compactness. The receivers are placed in room A. We consider n = 1, 4, 9, 16, 25 and 36, d = 0.5 λ, and ρ = 18 dB. The CCDFs for $C_{wf}(n)$ are plotted in Fig. 2 (solid lines). The rightward shift of the curves shows that $C_{wf}(n)$ increases with n, because space diversity provides additional spatial degrees of freedom for transmission. One performance indicator of interest is the capacity that can be supported 95% of the time, i.e. 5 % channel outage. Using a single antenna yields $C_{wf}^{0.05}(1)$ = 5.9 bps/Hz while MEAs with four antennas achieve $C_{wf}^{0.05}(4)$ = 20 bps/Hz, which is almost three and a half times larger. For n = 36, we can get as high as 106 bps/Hz.

The CDDFs of $I_{eq}(n)$ are also plotted in Fig. 2 (dashed lines). The advantage of having channel knowledge at the transmitter for water-filling to be employed is illustrated by the horizontal gap between the CCDFs of $C_{wf}(n)$ and $I_{eq}(n)$. For small n such as n = 4, the difference between $C_{wf}^{0.05}(4)$ and $I_{eq}^{0.05}(4)$ is only about 1 bps/Hz (about 5% difference). This gap increases with n, e.g. for n = 36, $C_{wf}^{0.05}$ is 11.3 % larger than $I_{eq}^{0.05}$.

The relative capacity gain of $C_{wf}(n)$ over $I_{eq}(n)$ is sensitive to ρ and n. $C_{wf}^{0.05}(n)/ I_{eq}^{0.05}(n)$ are plotted in Fig. 3. The gain decreases as ρ increases, and it decreases at a slower rate for larger n. When ρ is small, knowing the channel allows us to allocate power more efficiently to stronger subchannels and therefore achieve higher capacity as compared to equal power distribution over all subchannels. When ρ is large, there is sufficient power to be distributed over all sub-channels, therefore the relative strength of the subchannels become less important. For n = 4, the ratio decreases from 3 at ρ = -10 dB to 1 at ρ = 50 dB for $C_{wf}^{0.05}(n)/I_{eq}^{0.05}(n)$.

2. Asymptotic Behavior of MEA Capacities

We study how MEA capacity behave as n grows large in simulated channels. We only focus on the high SNR regime, ρ = 22 dB. Since $C_{wf}(n)/I_{eq}(n)$ is close to 1 for high SNR, we only consider water-filling capacity C_{wf}.

For simplicity, we consider linear arrays where the antenna-elements of MEA are equally spaced with two antenna spacings: d = 0.5 λ and 5 λ. The transmitting MEA is placed orthogonal to the long dimension of the

[1] Typical two sided power spectral density of thermal noise at 300 K (room temperature) for a receiver that is modeled as a 50 Ω resistance is -170.8dBm/Hz.

halfway (broadside arrangement as in [5]). We estimate the variance υ^2 and eigenvalues of the covariance matrix to compute C_{wf}* and C_{wf}^{o} using (9) and (15).

The average capacity $\overline{C}_{wf}(n)$ for different n is computed using 1000 realizations of H, and is plotted in Fig. 4 for d = 0.5λ and 5 λ. The lighter dashed lines are capacity approximated using the asymptotic growth rates for correlated case, i.e. straight lines with slope C_{wf}^{o}. The gap between simulation results and the asymptotic results grows smaller for increasing n. For d = 5 λ, $\overline{C}_{wf}(n)/n$ converges to 98 % of C_{wf}^{o} when n = 16. We observe that there is a consistently huge gap between $C_{wf}(n)$ from simulation and nC_{wf}* even for large antenna spacings, such as 5 λ. This is due to the correlation that is not captured by the independent fading assumption used to derive the asymptotic results in Section III-C-1.

If the assumptions in Section III-C-2 hold, and the correlation is correctly captured by our model, $C_{wf}(n)/n$ should converge almost surely to C_{wf}^{o} in the limit of large n. In the last figure, we illustrate this asymptotic behavior of $C_{wf}(n)/n$ at large SNR by plotting the empirical probability density functions (PDFs) of $C_{wf}(n)/n$ for n = 4, 9 and 16 with d = 0.5 λ (strong correlation between H_{ij}'s) and d = 5 λ (less correlation between H_{ij}'s). As n increases, the PDF becomes narrower and has a higher peak value, i.e. $C_{wf}(n)/n$ becomes less random. In the limit of large n, we expect the PDF of $C_{wf}(n)/n$ to converge to an impulse function centered at the value C_{wf}^{o}. The narrowing PDF's in Fig. 5 illustrate the almost-surely convergence of $C_{wf}(n)/n$ to C_{wf}^{o}. Note that when d = 5 λ, the PDF's are narrower and taller than when d = 0.5 λ. This indicates that the rate of convergence is higher when d is larger, which is the case when the correlation between H_{ij} is lower. Further analysis is needed to understand how correlation affects the validity of the asymptotic results in Section III-C when ρ is not large.

V. Conclusions

MEA systems offers potentially huge capacity gains over single-antenna systems. With perfect channel knowledge at the transmitter, water-filling solutions can be employed to achieve capacity C_{wf}. Equal power allocation is easier to implement, but this reduction in design complexity of the transmitter comes with a trade-off because I_{eq} can be significantly smaller than C_{wf}. The water filling gain C_{wf}/I_{eq} is most significant when the average received SNR ρ is small. $C_{wf}^{0.05}/I_{eq}^{0.05}$ = 3.5 when ρ = -10 dB, but at ρ = 50 dB, water filling gain is negligible, $C_{wf}^{0.05}/I_{eq}^{0.05} \approx 1$.

Assuming i. i. d. path gains between different antenna pairs, theoretical analysis shows that the capacity grows linearly with the number of antennas n in the limit of large n. However, in a more realistic propagation environment, correlation does exist between antenna pairs and causes a smaller rate of growth in capacity. Our simulation results show that for 0.5 λ antenna spacing, the simulated average capacity $\overline{C}_{wf}$ is only 79% of the predicted value nC_{wf}^{o} for n = 16 in the case of broadside with ρ = 22 dB. When the antenna spacing is increased, we see more agreement between C_{wf} and nC_{wf}^{o}. Indeed with d = 5 λ, $C_{wf}(n)/nC_{wf}^{o}$ = 98% when n = 16.

VI. Acknowledgments

The authors are grateful to Reinaldo Valenzuela, Jerry Foschini, Jonathan Ling and Dmitry Chizhik for allowing us to use their WiSE simulation tools, and for their valuable advice & suggestions. Discussions with Jack Salz and Da-shan Shiu have been enlightening and are much appreciated.

VII. References

[1] W. Jakes Jr., *Microwave Mobile Communications*, New Wiley, 1974.

[2] J. Winters, "Optimum Combining for Indoor Radio Systems with Multiple Users," *IEEE Trans. Commun.*, vol. com-35, no. 11, pp. 1222-1230, Nov. 1987.

[3] G. J. Foschini and M. J. Gans, "On Limits of Wireless Communication in a Fading Environment When Using Multiple Antennas," accepted for publication in *Wireless Personal Communications*.

[4] G. J. Foschini and M. J. Gans, "Capacity When Using Diversity At Transmit And Receive Sites and The Rayleigh-Faded Matrix Channel Is Unknown At The Transmitter," *WINLAB Workshop on Wireless Information Network*, New Brunswick, NJ, March 20-21, 1996.

[5] W. C. -Y. Lee, "Effects on Correlation Between Two Mobile Radio Base-Station Antennas," *IEEE Trans. on Communications*, vol. com-21, No.11, pp. 1214-1224, November, 1974.

[6] S. J. Fortune, D. H. Gay, B. W. Kernighan, O. Landron, R. A. Valenzuela and M. H. Wright, "WiSE design of Indoor Wireless Systems: Practical Computation and Optimization," *IEEE Computational Science and Engineering*, vol. 2, no. 1, pp. 58-68, March, 1995.

[7] G. J. Foschini and R. A. Valenzuela, "Initial Estimation of Communication Efficiency of Indoor Wireless Channels," *Wireless Networks*, vol. 3, no. 2, pp. 141-54, 1997.

[8] T. M. Cover and J. A. Thomas, *Elementary of Information Theory*, John Wiley & Sons, New York, 1991.

[9] I. E. Telatar, "Capacity of Multi-antenna Gaussian Channels," submitted to *IEEE Transactions on Information Theory.*

[10] A. M. Khorunzhy, B. A. Khoruzhenko and L. A. Pastur, "Asymptotic properties of large random matrices with independent entries," *Journal of Mathematical Physics*, vol. 37, no. 10, pp. 5033-60, Oct. 1996.

[11] Y. Q. Yin, "Limiting Spectral Distribution for A Class of Random Matrices," *Journal of Multivariate Analysis*, vol. 20, pp. 50-68, 1986.

[12] Jack Silverstein, "Strong Convergence of the Empirical Distribution of Eigenvalues of large Dimensional Random Matrices," *Journal of Multivariate Analysis*, vol. 55, no. 2, pp. 331-339, 1995.

[13] David Tse, "Capacity Scaling in Multi-antenna Systems", in preparation.

VIII. Figures

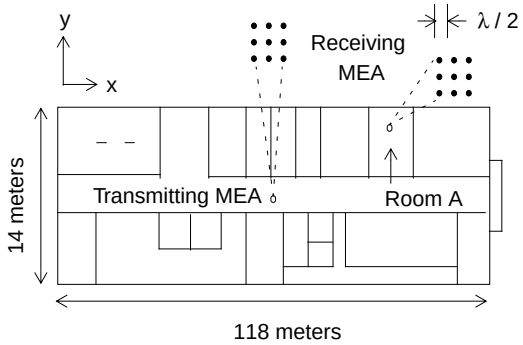

Fig. 1. Floor Plan for the office building modeled in WiSE. The transmitting MEA is placed with its adjacent sides parallel to x-axis and y-axis, respectively. The receiving MEA is placed with random orientation at each of the sample location in room A.

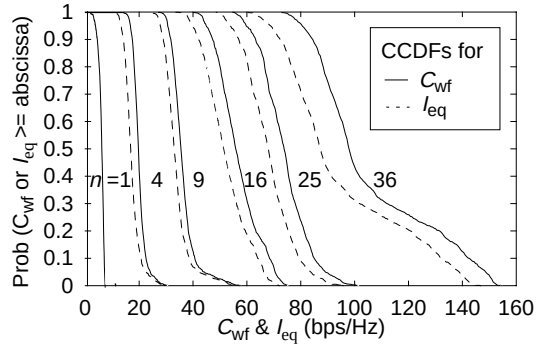

Fig. 2. The CCDFs of C_{wf} (achieved via water -filling) and I_{eq} (with equal power allocation) for n = 1, 4, 9, 16, 25 & 36 at received ρ = 18 dB. MEA antennas are arranged in square grids with d = 0.5 λ.

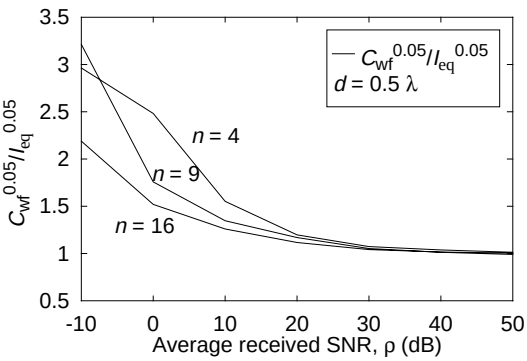

Fig. 3. Water-filling gain $C_{wf}^{0.05}/I_{eq}^{0.05}$ (solid lines) over varying average received SNR, ρ, in room L147 for n = 4, 9 and 16. Antennas at both the transmitter and the receiver are arranged in square grids in this case.

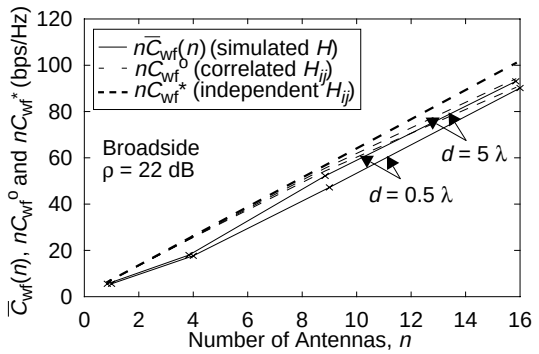

Fig. 4. The average capacity $\bar{C}_{wf}(n)$ is plotted against n. We consider linear arrays with the transmitting MEA placed parallel to the y-axis (broadside case). nC_{wf}^{*} and nC_{wf}^{o} are asymptotic results for correlated and independent H_{ij}, respectively (Section III-C).

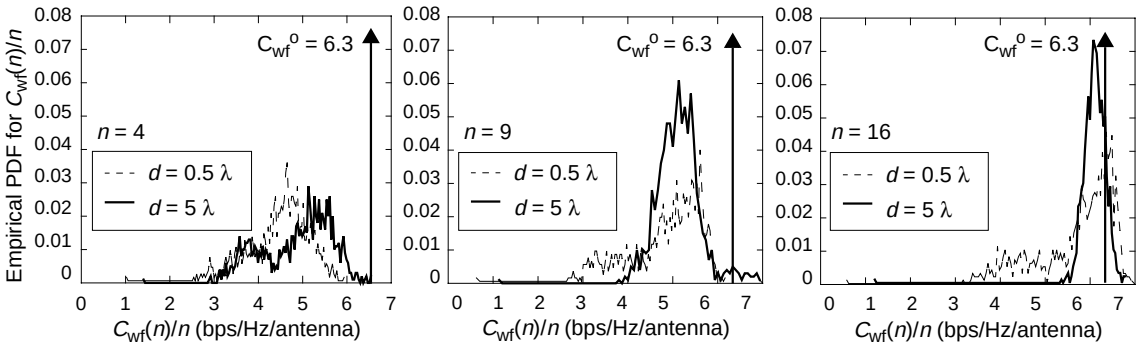

Fig. 5. Empirical probability density function of the normalized capacity $C_{wf}(n)/n$ for n = 4, 9 and 16. We consider linear arrays with antenna elements separated by 0.5 λ and 5 λ. The reference value is C_{wf}^{o} as predicted by the asymptotic theory considering correlated H_{ij}'s.